sciendo Slovak Journal of Civil Engineering
Vol. 33, 2025, No. 1, 44 – 54
DOI: 10.2478/sjce-2025-0005

NUMERICAL STUDY OF SHALLOW ROCKING FOUNDATIONS UNDER SEISMIC EXCITATION AND LATERAL MONOTONIC LOADINGS

Seyed Omid, KHAMESI[1]*, Seyed Majdeddin, MIR MOHAMMAD HOSSEINI[1]

Abstract

Recent studies have shown that the rocking of foundations and the yielding of soil can decrease the load transmission to a superstructure during earthquakes. However, more investigations should be carried out to make this design philosophy a practical solution among seismic engineers. The research presented applies the finite element method to study the response of single-degree-of-freedom systems constructed on soils of medium density with rocking foundations prone to lateral monotonic and ground motion loadings. Various dynamic analyses were performed in order to explore the role of two influential parameters, i.e., the static safety factor versus the soil's bearing capacity failure and the structure's slenderness ratio, in the performance of a soil-foundation system and the structure's stability. A comparison of the system's behavior for the two loading cases is also presented. According to the results, the geometric nonlinearity (the foundation's detachment from the underlying soil) and the material nonlinearity responses are evident from the analyses. Also, the dominant role of the foundation's safety factor versus the vertical loads in the system's performance has been found to be indisputable.

Address

[1] Department of Civil and Environmental Engineering, Amirkabir University of Technology, Tehran, Iran

* ***Corresponding author:*** okhameis@aut.ac.ir

Key words

- Rocking foundation,
- Rocking isolation,
- Soil-structure interaction,
- Dynamic analysis,
- Finite element method,
- Numerical model,
- Earthquakes.

1 INTRODUCTION

Engineers aim to design earthquake-resistant structures in regions with high seismic activity. However, it has been found that a structural system's safety does not necessarily improve from increasing its strength. As a result, design philosophies have been developed in order to control seismic damage and achieve a safe rupture. To this end, structural systems have been established such that the failure of some elements under a heavy load does not result in the whole structure's collapse because the remaining members create alternative paths for transmitting the loads. Although many research projects have been carried out to develop structures with such behavior, the study of a soil-structure performance as a system is mostly ignored because the current design principles are basically related to the superstructure, and the impact of the soil and foundation is underrated (Anastasopoulos et al., 2010).

Many studies show that the nonlinear performance of soil under dynamic loads is inevitable and can be favorable (Gajan and Kutter, 2008; Anastasopoulos et al., 2010; Deng et al., 2012; Antonellis and Panagiotou, 2014). As a result, the rocking isolation concept has been introduced (Anastasopoulos et al., 2010). According to this new approach, structures are designed with rocking foundations, and the footings are allowed to move relative to the underlying soil. Contrary to the conventional design method, the ductility and formation of plastic hinges in structures with rocking foundations are shifted from the structure itself onto the underlying soil. The soil-foundation system's yield is therefore applied to protect the superstructure.

Despite the necessity for and benefits of using a new method for foundation design, consideration of the rocking isolation approach for construction projects has been avoided due to the lack of knowledge about the performance of systems with rocking foundations under seismic excitation. Moreover, there are still uncertainties concerning the estimation of permanent deformations of a foundation after an earthquake.

The present research investigates the performance of the soil-foundation interaction for a simple bridge or structure, which has been idealized as a single-degree-of-freedom system (SDOF) with a shallow rocking foundation constructed on medium density soil, by applying the finite element method. Fig. 1 shows a schematic diagram of the system studied. It basically consists of a shallow foundation supporting an elevated mass.

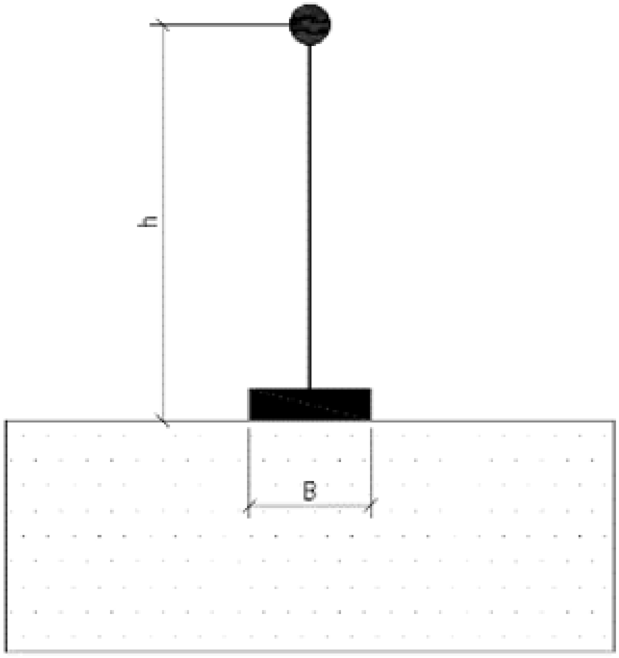

Fig. 1 *The schematic diagram of a single-degree-of-freedom system (SDOF)*

The main objectives of our research are to demonstrate a full-range soil-foundation performance during rocking and investigate the differences in the system's performance for different static safety factors and the structure's slenderness ratios (the ratio of the structure's height to the width of its foundation). Accordingly, the numerical model has been verified against the results from an experimental study conducted at the Amirkabir University of Technology (Sharifzadeh Asli et., 2018). After validating the model, the structure was subjected to increasingly monotonic horizontal displacements until its collapse. The results from the monotonic analyses are compared with those from the next stage of the study, i.e., evaluating the system under seismic base excitations. The analyses are carried out for different vertical safety factors against bearing capacity failure (FS_v) and structures with various slenderness ratios (h/B) to study the performance of the system due to these parameters.

2 BACKGROUND

Housner's (1963) pioneer research was conducted for rigid blocks on rigid bases under free vibration, constant acceleration, sinusoidal acceleration, and the earthquake's motion. It was among the first investigations performed to get an insight into the rocking foundation phenomenon. Housner (1963) studied the overturning potential of rigid blocks. He showed the stability of a tall, slender block subjected to an earthquake is much greater than an identical block under a constant horizontal force. Nevertheless, the inelastic behavior of some parts of soil, even under static conditions, is inevitable. As a result, the formation of failure surfaces and severe inelastic soil responses are expected for a system subjected to seismic motion. In order to study structures on inelastic soil, numerical and experimental methods are available. Centrifuge tests (Ko et al., 2018), 1g shaking tables (Tsatsis and Anastasopoulos, 2015), single-degree-of-freedom systems with a slow cyclic loading laboratory test (Anastasopoulos et al., 2012), and field experiments (Algie et al.,2010) are the main physical modeling approaches. Numerical methods include a beam on a nonlinear Winkler foundation (BNWF) (Antonellis and Panagiotou, 2014), inelastic macroelements (Chatzigogos et al., 2011), and continuum models using finite difference or finite element techniques (Torabi and Rayhani, 2014). In recent years, owing to advanced computer systems and calculation software, applying the finite element method to investigate rocking foundations has improved (Gelagoti et al., 2012; Kourkoulis et al., 2012; Panagiotidou et al., 2012; Gazekas et al., 2013). These studies confirmed the pronounced role of static safety factors against bearing capacity failure on the behavior of rocking foundation systems. However, few numerical studies in the literature consider actual seismic records for the system. Moreover, the investigation of important parameters, such as a structure's slenderness ratio, is neglected in most studies, especially those under seismic excitation.

The research herein considers various static foundation safety factors and slenderness ratios of structures for systems with rocking foundations constructed on inelastic medium dense soil. The performance of these systems is studied under a real earthquake record.

3 ANALYSES ASSUMPTIONS

The soil type, structural specifications, and loading properties are the most influential items in a soil-structure interaction problem. Other factors, such as the simplification of the numerical model and interface characteristics, also have an effect on behavior, but their impact is lower. Some assumptions have been made to decrease the number of factors affecting the results. For the current research, the main assumptions are as follows:

3.1 Soil properties

Medium dense soil was selected as the single-layered underlying soil, with a friction angle of φ = 33° and a cohesion value of c = 15 kN/m^2. The soil layer was considered isotropic and homogeneous. The site has no groundwater, and the soil is unsaturated. Tab. 1 shows the soil properties considered.

Tab. 1 *Geotechnical parameters of the site selected*

Soil Type	φ°	c (kN/m²)	E (MPa)	ν	ρ (kg/m³)	G (MPa)
Medium dense	33	15	60	0.3	1600	23.1

3.2 Structural Properties

The structure consists of an elevated mass connected to a shallow foundation with a pier. This idealization could be rational for a bridge or simple structure. Since the paper mainly focuses on geotechnical fields, the superstructure and foundation were considered to be rigid.

3.3 Loading pattern

This research used two loading patterns, i.e., lateral monotonic and real seismic excitation. The monotonic loading was exerted by applying horizontal displacements to the lumped mass of the system in a displacement-controlled manner. The Kobe 1995 earthquake (Takatori record) was selected as the seismic excitation for the dynamic analyses. This record represents a severe seismic event. Such massive ground motion is beyond the design earthquake properties in many areas and resembles the unpredicted earthquakes with unknown faults that may occur in areas with a high seismic risk. The acceleration time history of the record is shown in Fig. 2. To explore the effect of an earthquake's intensity, the record was scaled to 0.1g, 0.3g, and 0.6g PGA values.

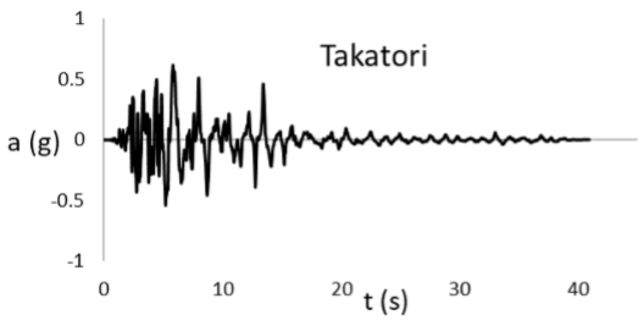

Fig. 2 *Acceleration time history of the Takatori record (Kobe earthquake)*

4 NUMERICAL MODEL

Explicit nonlinear finite element (elasto-plastic) analyses were carried out using ABAQUS software. Due to the high number of numerical analyses and the computational efforts involved, two dimensional models were used. The soil was simulated by means of four-noded plain-strain elements (CPE4). The foundation and superstructure were modeled using rigid elements. Contact between the foundation and the underlying soil was simulated using the software's contact pair option, so detachment of the foundation from surrounding soil was possible during the analysis. The properties of both the normal and tangential directions of the contact can be defined. A "hard-contact" relationship was applied for the normal direction, and the tangential behavior was described through the "penalty friction" option.

The model's dimensions were determined through a trial-and-error process. So, the seismic loads were applied to models with different dimensions. The model with the smallest dimensions, which showed the minimum effect on the model's response (stress and deformation), was chosen as the optimum size. The model's width almost equaled 30B (B is the foundation's width). Semi-infinite elements were adopted for the model's lateral boundaries to absorb any energy from the earthquake and avoid wave reflection from the boundaries into the model. Fig. 3 shows one of the models used for the finite element analyses. The model consists of about 5,000 elements. Smaller elements were used for modeling the soil adjacent to the foundation, and larger elements were applied for further locations of lesser concern. The underlying soil was simulated using the Mohr-Coulomb constitutive model. Equation 1 describes the failure criterion for the model:

$$\tau=\sigma_n \tan\phi + c \qquad (1)$$

In this equation, τ represents the soil's shear strength; σ_n is the plane's normal stress; and the φ and c parameters indicate the soil's angle of internal friction and cohesion, respectively. The model's parameters were selected according to Tab. 1. Rayleigh damping was also introduced into the models, with the following equation:

$$[C]=\alpha[M]+\beta[K] \qquad (2)$$

In equation [C], [M] and [K] represent the damping, mass, and stiffness matrices of the system, respectively. α and β are the Rayleigh damping coefficients. Assuming the soil system's damping is equal to 5%, the values of these coefficients were calculated and applied to the numerical model (α= 0.826281, β = 0.00226917).

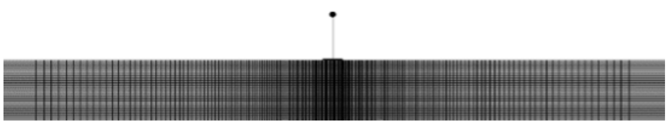

Fig. 3 *A typical model (geometry and FE mesh) used for the numerical analyses*

5 VALIDATION OF THE MODEL

For the purpose of the verification of the model, the results from a single-degree-of-freedom (SDOF) physical model were used. This physical model was developed at the Soil Mechanics Laboratory of Amirkabir University of Technology to evaluate the rocking isolation phenomenon (Sharifzadeh Asli et al, 2018).

5.1 Description of the physical model

The physical model was composed of the following sections: the superstructure, the vertical loading system, the horizontal loading system, the testing tank, and the underlying soil. The tests were conducted on a relatively tall SDOF structure with a structural height to-foundation width ratio of h/B = 3 and a scale factor of 1/20. The laboratory model represents a structure with a 9 m height and a foundation width of 3 m. Dry silica sand was utilized as the underlying soil for the study. The soil properties are according to Tab. 2.

Tab. 2 *The properties of soil used for the physical modeling (Sharifzadeh Asli, 2018)*

Soil	Dry Silica sand
Specific Gravity	2.67
Mean Grain Size, D_{50} (mm)	1.643
Coefficient of Uniformity, C_u	1.63
Maximum Dry Unit Weight (kN/m^3)	16.79
Minimum Dry Unit Weight (kN/m^3)	14.4
Relative Density (%)	60
Friction Angle (Deg.)	33

The center of the lumped mass was subjected to low periodic lateral displacements during the tests. The loading cycles consisted of four phases. For the first three phases, each included ten cycles with a constant amplitude of δ/δ_R = 0.05, 0.1, and 0.3, respectively (δ_R = 7.5 cm is the displacement of the model's center of mass, which would topple it to on the rigid subgrade). For the 4th phase, the displacement amplitude increased by a rate of 2.5 mm/cycle until the model's collapse. The displacement pattern applied is shown in Fig. 4 (Sharifzadeh Asli et al., 2018).

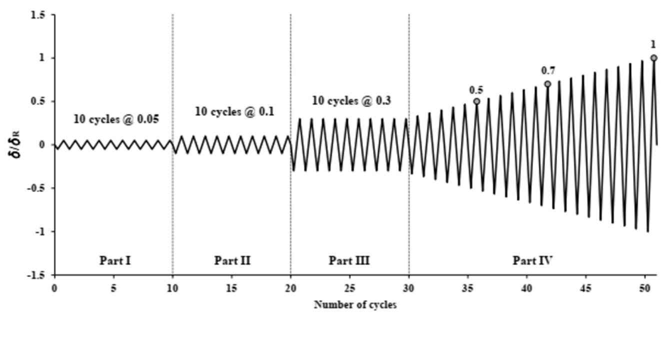

Fig. 4 *The lateral displacement pattern applied to the model's lumped mass (Sharifzadeh Asli et al., 2018)*

5.2 Comparison between the numerical analysis and experimental test results

The experimental programs include three soil compaction levels (loose, medium, and dense) and six different structural masses. In the present study, the test program with medium dense soil and a structural mass equal to 80.2 kg was considered for the purpose of verifying the numerical model. The properties of the physical model described are turned into their prototypical values using the scale coefficients presented in Tab. 3. As mentioned earlier, the physical model scale factor is 1/20, so for the current investigation, N = 20. The experiments have shown that the exponent α might be of the order of 0.5 for the sand and 1 for the clay (Sharifzadeh Asli et al., 2018).

A comparison between the results calculated and those from the experiments is illustrated in Fig. 5 in terms of dimensionless moment-rotation and settlement-rotation graphs. The settlements were normalized by dividing them by the foundation's width (B). Also, the moments and rotations were normalized by dividing them by $M_R = mgB/2$ and $\varphi_R = \tan{-1}(B/2H_{CM})$, which represents the overturning moment and the toppling rotation of the system's equivalent rigid block placed on a rigid foundation, respectively. Where H_{CM} is the height of the center of the mass, as can be seen, the values for the settlement and moment, calculated through the finite element model and obtained from the experimental test, are in good general agreement. The trends for several loading cycles are fairly similar, which indicates the accuracy of the assumptions and methods applied during the numerical analysis.

Tab. 3 *Scale coefficients for the physical modeling (Sharifzadeh Asli et al., 2018)*

Quantity	Dimension	Scale factor (Model quantity/ Prototype quantity)	
		In general	1-g Condition (Physical laboratory models)
Length	[L]	n_l	N^{-1}
Mass density	[M].[L^{-3}]	n_ρ	1
Gravity	[L].[T^{-2}]	n_g	1
Stiffness (for soil)	[M].[L^{-1}].[T^{-2}]	n_G	$N^{-\alpha}$
Mass	[M]	$n_\rho n_l{}^3$	N^{-3}
Time	[T]	1	1
Force	[M].[L].[T^{-2}]	$n_\rho n_g$ nl ^{3}	N^{-3}
Stress	[M].[L^{-1}].[T^{-2}]	$n_\rho n_g n_l$	N^{-1}

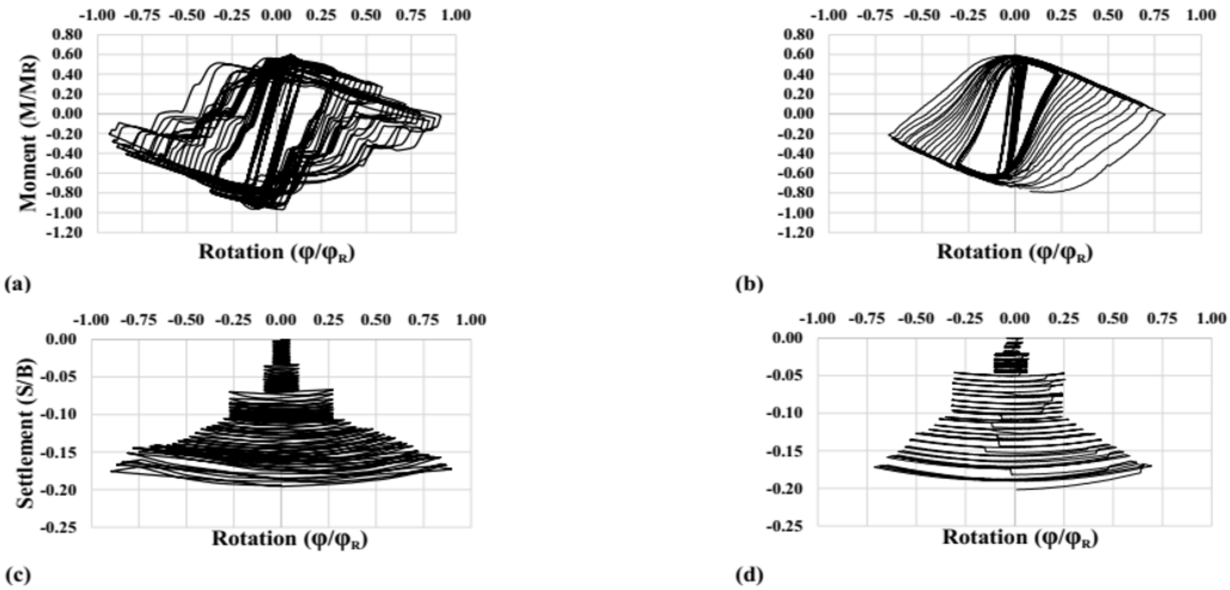

Fig. 5 *(a) Normalized moment-rotation graph from the FEM analysis, (b) Normalized moment-rotation graph from the experiment (Sharifzadeh Asli,2018), (c) Normalized settlement-rotation graph from the FEM analysis, (d) Normalized settlement-rotation graph from the experiment (Sharifzadeh Asli,2018)*

6 ROCKING UNDER MONOTONIC HORIZONTAL LOADING

This section studies the performance of a system under monotonic lateral loading conditions. Pushover analyses were carried out by applying a horizontal displacement to the lumped mass of the system. The effect of two important parameters, i.e., the safety factor against the vertical loads (FS_v) and the slenderness ratio (h/B), on the structure's behavior were investigated during the analyses. The ratio of the foundation's ultimate vertical load capacity (N_{ult}) to the vertical load applied (N = mg) has been expressed through the safety factor against the vertical loads or static safety factor ($FSv = N_{ult}/N$).

6.1 The effect of the safety factor

Three static safety factors against vertical loads (FS_v) were considered for the investigation: FS_v=1.25, FS_v=2, and FS_v=5. Besides FS_v= 2, two other safety factors were chosen to represent two ultimate loading cases. FS_v=1.25 shows the heavily loaded systems, and FS_v=5 represents conservatively designed cases, i.e., lightly loaded systems. Tab. 4 shows the vertical load levels for these different static safety factors.

Tab. 4 *Vertical loads (N) applied and ultimate vertical load capacity (Nult) of the system for three cases of static safety factors*

FSv	N (kN)	N_{ult} (kN)
1.25	2899.2	3624
2	1812	3624
5	724.8	3624

The vertical loads were applied to the system through altering the structure's lumped mass value (m). The bearing capacity of the foundation was calculated using Hansen's equation (Bowles,1977):

$$q_{ult}=cN_c\,S_c\,d_c\,i_c\,g_c\,b_c+qN_q\,S_q\,d_q\,i_q\,g_q\,b_q+0.5\gamma BN_\gamma\,S_\gamma\,d_\gamma \qquad (3)$$

In this equation, γ, c and B are the soil's specific weight and cohesion and the foundation's width, respectively. Parameter q represents the vertical pressure of the soil at the foundation's bottom level and the surcharge (if any) applied. N_c, N_q and N_γ were calculated according to equations (4), (5) and (6), while ∅ represents ∑. Other parameters in equation (3) are the shape (S), depth (d), load inclination (i), and the ground (g) and base factors (b), which can be extracted from tables provided in Bowles (1977) (discussing them is out of the scope of the current paper).

$$N_q = e^{\pi \tan\emptyset}\tan^2(45+\tfrac{\emptyset}{2}) \qquad (4)$$

$$N_c = N_q \cot\emptyset \qquad (5)$$

$$N_\gamma = 1.5(N_q-1)\tan\emptyset \qquad (6)$$

The moment-rotation diagrams of systems under monotonically increasing horizontal displacement for the three static safety factors are shown in Fig. 6. As illustrated, maximum value for the moment capacity belongs to the system with a safety factor FS_v=2. It complies with other research projects for systems constructed on clay (Panagiotidou et al., 2012; Gazetas, 2015). The moment capacity for the two other safety factors is almost equal. The maximum moments are reached at relatively small rotations, when the system's uplift begins. The rotation angle at the instant of a collapse (the toppling rotation) is in relation to the safety factor. The toppling rotation increases as the safety factor increases, which demonstrates a more desirable structural response.

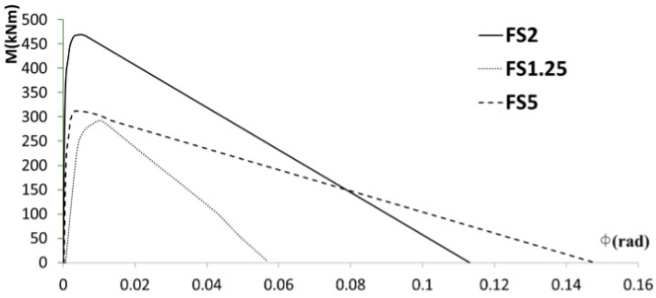

Fig. 6 *The moment-rotation graphs under monotonic lateral loading for various safety factors (h/B=3)*

The soil plastic deformation contours at the instant of imminent collapse for the three safety factors considered (FS_V=1.25, 5 and 5) for the h/B = 3 system are shown in Fig.7. The foundation does not uplift from the underlying soil for the system with relatively low safety factors (FS_v=1.25). In this case, plastic deformations were observed in large areas of the soil, so the behavior was strongly inelastic. Accordingly, the failure results from the insufficient bearing capacity of the foundation. When the safety factor is relatively large (FS_v=5), the structure experiences large rotations and a significant uplift of the foundation at the instant of the collapse. The foundation and the underlying soil connect in a small area. Also, the soil plasticity only occurs in a confined zone adjacent to the foundation's edge. The uplifting of the system is the dominant mode of failure in this case. Thus, two main failure mechanisms are observed for systems with a rocking foundation, depending on the vertical loading intensity. For the FS_v=2 case, the foundation uplift from the underlying soil occurs for a small part of the footing, and the plastic deformations exist in more areas of the soil compared to the FS_v=5 case. However, these plastic zones are less extended than the FS_v=1.25 case. As a result, the performance would be a combination of yielding soil and an uplifting foundation.

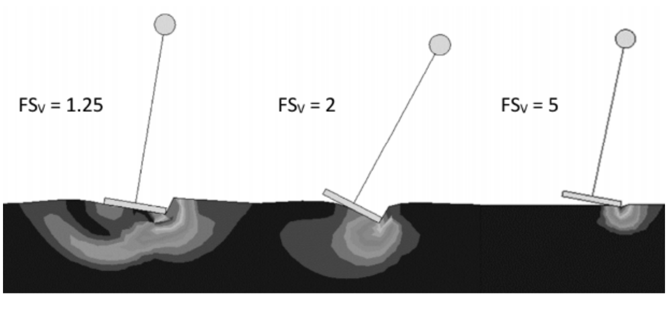

Fig. 7 *Plastic deformation contours in the soil at the instant of collapse for the three safety factors studied (h/B = 3)*

6.2 The structure's slenderness ratio effect

Another influential factor in soil-foundation interaction behavior, which is usually neglected in rocking foundation studies, is the structure's slenderness ratio (the ratio of the structure's height to the width of its foundation). Numerical analyses have been conducted to investigate the effect of this parameter on the foundation's rocking response. Accordingly, slenderness ratios (h/B) ranging from 1 to 10 were considered. The models were also analyzed for various vertical loads of superstructures to cover a full range of safety factors. Fig. 8 shows the moment-rotation graphs obtained from finite element analyses for the three safety factors against vertical loading (FS_v=1.25, 2, 5) and the h/B=1, 5, and 10 slenderness ratios.

As seen in the Fig. 8 graphs, as the slenderness ratio increases, the moment capacity of the system decreases due to the more pronounced role of the P-δ effect for slender systems, in which the moment is the principal influential factor for their stability. The moment capacity reduction is more apparent for foundations with low safety factor values. The reason is that, for lightly loaded systems (large safety factor values), the P-δ effect has a low effect on the moment's capacity value. The soil does not show plastic behavior for these systems; hence, the moment capacity is achieved at relatively small rotations. Since the P-δ effect requires rotations to develop, its role is not substantial for systems with low rotation values. In contrast, for heavily loaded systems experiencing massive soil plastification, the moment capacity is reached at larger rotations; as a result, the P-δ effect is more significant.

Fig. 9 shows the dimensionless toppling rotations (φt / φ_r) versus the normalized vertical load ($N/N_{ult}=1/FS_V$) for a number of slenderness ratios. The toppling rotations are normalized with respect to the toppling rotation of the equivalent rigid block on a rigid base ($\varphi_r = \tan^{-1}B/2h$). The detrimental role of P-δ effects can also be inferred from the Fig. 9 graphs. For all the slenderness ratios, as described in the previous section, with an increasing vertical load (a declining safety factor), the φ_t / φ_r ratio decreases, and the system topples in smaller rotations. As mentioned earlier, the role of the p-δ effects is more remarkable for heavily loaded systems. Hence, the toppling rotation approaches zero when the safety factor is near 1. Indeed, due to extensive soil's plastic behavior occurring under vertical loading, even small rotations can cause toppling and failure of the system. To the contrary, for large safety factor values, the toppling rotation tends to be like those of the equivalent rigid block on a rigid base due to the limited soil plasticity.

The slenderness ratio is also effective on a dimensionless toppling rotation. This effect is more pronounced for heavily loaded systems, where the soil's nonlinear behavior is dominant. Thus, the effect of the h/B ratio would be insignificant for a lightly loaded system in which the soil response is almost elastic.

For a constant safety factor value (FS_V), as the slenderness ratio increases, the normalized toppling rotation (φt /φr) decreases, and the system collapses at smaller rotation angles. This phenomenon can be attributed to the different failure mechanisms of slender systems compared to short systems (a low value of the h/B ratio). For high values of h/B ratios (slender systems), the overturning moment controls the foundation's performance; as a result, the failure mechanism is rotational. However, a horizontal translation is more effective on failure than on rotation for short systems.

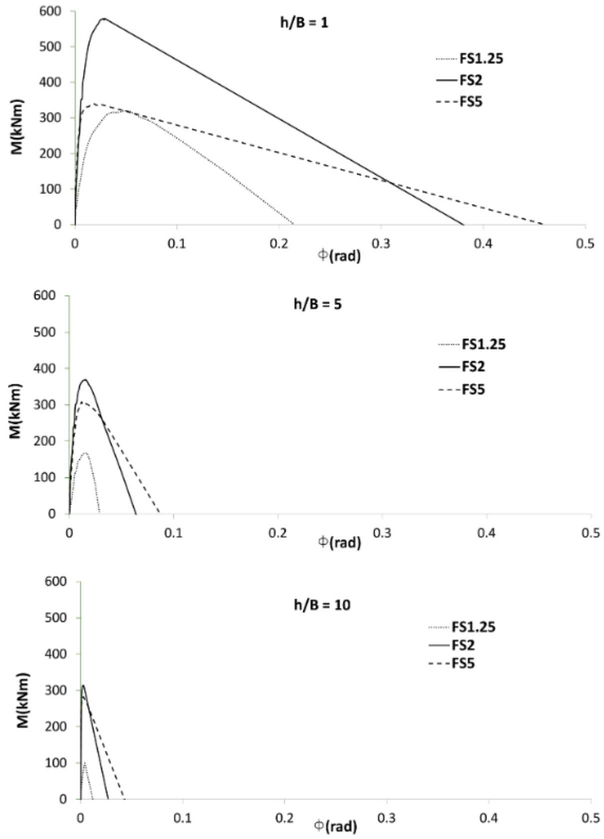

Fig. 8 *The moment-rotation graphs for the three slenderness ratios and various safety factors*

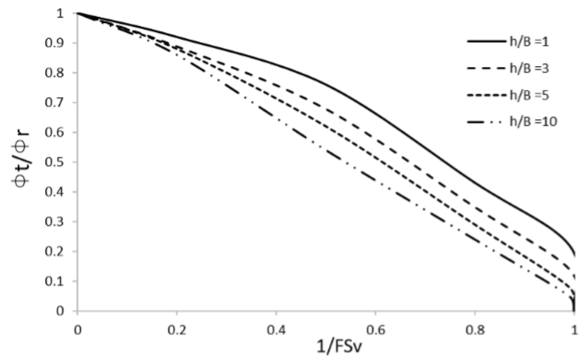

Fig. 9 *The dimensionless toppling rotation as a function of the safety factors and slenderness ratio*

7 ROCKING UNDER SEISMIC EXCITATION

The performance of the SDOF system was investigated under seismic excitations in this section by applying the scaled acceleration time histories of the Takatori record (PGA=0.1g, 0.3g, and 0.6g). The results from the dynamic analyses conducted and their further development are presented here.

7.1 The effect of the safety factor

Fig. 10 shows the moment-rotation graphs for the three safety factors against the vertical loading FS_v=1.25,2 and 5, respectively, and the three scaled Takatori records, i.e., PGA = 0.6g, PGA =0.3g, and PGA =0.1g. The diagrams of the monotonic lateral loading cases are also presented for comparison.

When the safety factor is the minimum (FS_v=1.25) for all the PGA values, the hysteresis loops are well beyond the monotonic loading curves. For PGA=0.6g and 0.3g, the soil undergoes large deformations, and after demonstrating heavy inelastic behavior, failure of the bearing capacity occurs. Toppling of the system is also evident in these motion intensities. Of course, for the PGA = 0.1g case, the soil behavior is rather elastic due to the low intensity of the ground motion, and the collapse of the system is not observed.

For the highest safety factor value (FS_v=5), the moment-rotation hysteresis loops are enveloped by the monotonic loading curves in all the motion intensity values studied. In this case, unlike the former, the curves are symmetric, and residual deformations are not observed. The performance of the system when the safety factor equals 2 (FS_v=2) is somewhat between the two other cases explained. For the seismic motion intensity with PGA = 0.1g, the hysteresis loops are confined by the monotonic loading curves, and the behavior is near the lightly loaded case (FS_v=5). However, for the PGA = 0.3g and PGA = 0.6g motion intensity cases, the performance is comparable to the heavily loaded case (FS_v=1.25). Accordingly, large deformations and failure of the bearing capacity mechanisms followed by toppling of the structure are observed for the PGA = 0.6g case. Remarkably, for the PGA = 0.3g, a collapse does not happen despite the residual rotations and tilting of the foundation. The earthquake's transient and oscillating nature is helpful in this case and prevents the system from overturning in some critical moments. As expected, the incremental intensity of the motion increases the soil-foundation's nonlinear performance for all the safety factors.

7.2 The structure's slenderness ratio effect

Dynamic analyses were carried out for the PGA = 0.6g scaled Kobe acceleration time history to investigate the impact of the slenderness ratio on the system's performance under seismic excitation. Fig. 11 demonstrates the moment-rotation graphs for two extreme cases of slenderness ratios, i.e., h/B=1 and h/B=10, when the foundation's safety factors are FS_v=1.25 and FS_v=5.

When comparing the h/B=1 and 10 slenderness ratios for the FS_v =1.25 value, the effect of the p-δ on the system's performance is visible. The effect is negligible for the system with h/B=1. An oscillation with a high amplitude of rotations was observed without any substantially permanent tilting and toppling. But, for the h/B=10, the system began tilting with the low rotation values and eventually collapsed. In the FSv=5 case, due to the dominant uplifting behavior in the systems with high FSv, the residual rotation was lower for the slender structure (h/B=10) compared to the FSv=1.25 case, and the toppling did not occur.

The variations of the moment capacity for the different slenderness ratios and safety factors demonstrated the same patterns presented by the monotonic analysis case, i.e.,

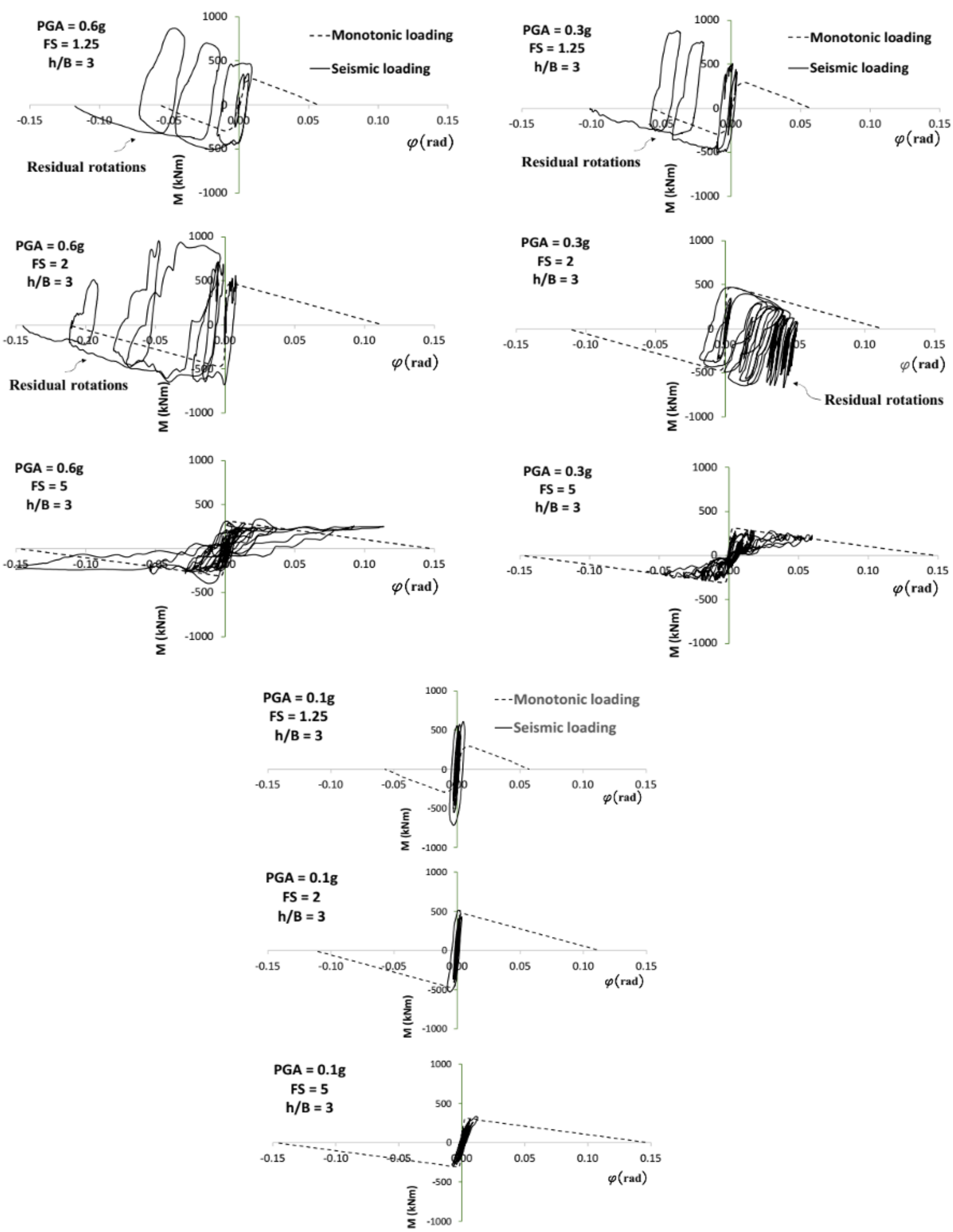

Fig. 10 *Moment-rotation diagrams for systems with three different static safety factors under the scaled Takatori records*

as the slenderness ratio increased, the moment capacity reduced. This reduction was more evident for the heavily loaded systems than the lightly loaded foundations due to the role of the p-δ effects, as described before.

As seen in Fig. 11, the toppling rotation value for the FS_v=1.25 and h/B=10 case was less than the FS_v=1.25 and h/B = 3 case (Fig. 10). These results also complied with the findings from the monotonic loading analyses presented earlier and was due to the governing rotational failure mechanism for the slender systems.

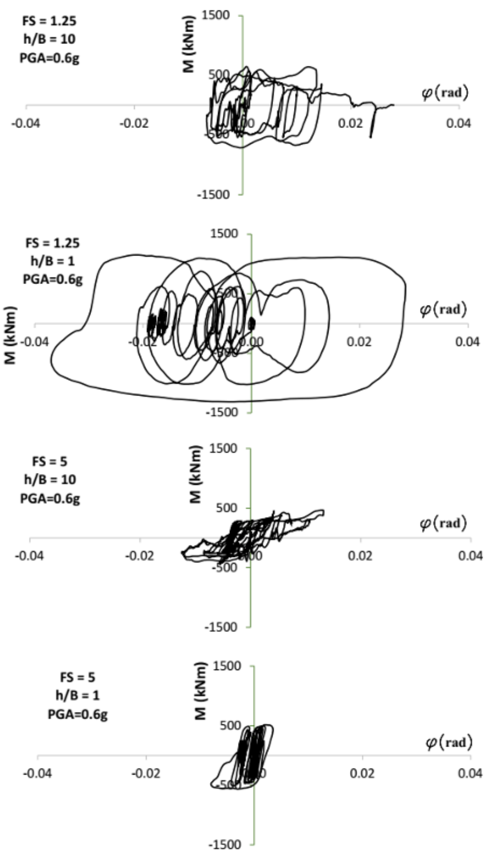

Fig. 11 *Moment-rotation diagrams for two extreme cases of slenderness ratios and static safety factors under the PGA=0.6g scaled Takatori records*

7.3 The vertical displacement of the foundation (settlement and uplift)

Fig. 12 shows the settlement-rotation graphs (the negative values represent the foundation's settlement) obtained from the dynamic analyses for the two extreme safety factors (FS_v=1.25 and FS_v=5), according to the two scaled Takatori earthquake records (PGA = 0.1g and 0.6g). The foundation's settlement due to the monotonic loading is also presented for comparison. The settlements were calculated beneath the center of the foundation. For the FSv=1.25 case, the system's collapse is apparent for the PGA=0.6g case, where the accumulating settlements accompanied by the residual tilts of the foundation occurred.

Small foundation uplifts were observed for the system with FS_v=5 under seismic excitation with PGA=0.6g. However, as time passed, the accumulation of the settlement took place under the repeated dynamic loading cycles. Unlike the PGA=0.1g case, there was no similarity between the monotonic analysis and seismic analysis curves. The effect of the earthquake's intensity on the system's performance is evident through the larger settlement values and the permanent foundation tilts for the PGA = 0.6g scaled ground motion for both safety factors studied.

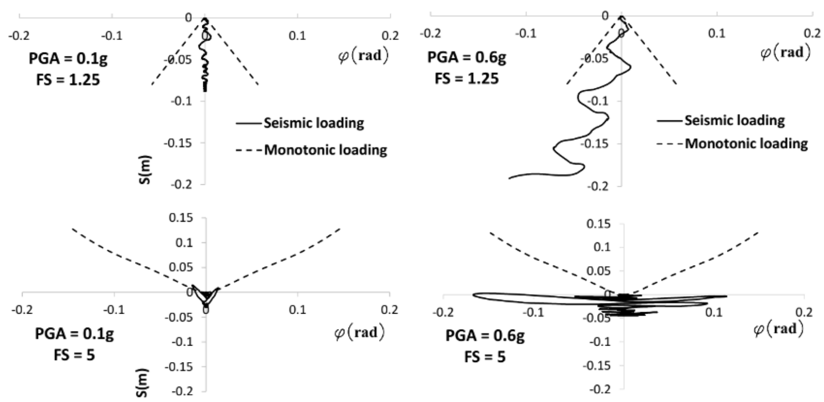

Fig. 12 *The settlement-rotation graphs for the two extreme safety factor cases under two scaled Takatori recordss*

8 SUMMARY AND CONCLUSIONS

The rocking performance of shallow foundations on medium dense soil was numerically investigated. Single degree-of-freedom (SDOF) systems were analyzed under lateral monotonic loading and seismic excitation using the finite element method. The numerical model was verified against the results from a series of laboratory experiments conducted to study rocking foundations at the Amirkabir University of Technology. During the finite element analyses, the impact of the safety factor against the vertical loads ($FS_v = N_{ult} /N$), the structure's slenderness ratio (h/B), the P-δ phenomenon, and the earthquake's intensity on the system's behavior were studied. The value of the structure's lumped mass was changed during the analysis in order to apply different vertical loads and obtain different static safety factors. The most important results are as follows:

- The safety factor against vertical loads is the main parameter that controls whether the uplifting of the system from the supporting soil or the failure of the soil's bearing capacity is the prevailing performance. Lightly loaded systems (high FS_v values) experience the uplifting of the foundation under lateral loadings. For heavily loaded systems (low FS_v values), soil plastification and mobilization of soil's bearing capacity failure predominate. The intensity of the seismic motion is the second factor affecting the system's behavior mode (uplifting or soil's bearing capacity failure mechanism). Obviously, as the ground motion intensity increases, the yielding of the soil becomes the system's principal behavior approach.

- The structure's slenderness ratio (h/B) is another important parameter in the investigation of the rocking foundation. The moment capacity of the system decreases by increasing the slenderness ratio due to the role of the P-δ effect, which becomes more crucial for slender systems. However, this response is not pronounced for the FS_v=5 cases. The P-δ effect has a detrimental role on the system's stability and facilitates the collapse of structures. Nevertheless, the safety factor value also controls the severity of this influence. Due to the soil yielding and larger rotation values for heavily loaded systems, the P-δ effects are more pronounced than for the lightly loaded systems.

- The foundation settlement under monotonic and seismic loading also depends on the safety factor against vertical loading and the earthquake's intensity. For low values of FS_v, the foundation's center undergoes accumulating settlement in both monotonic and seismic excitation load cases. Lightly loaded foundations (high values of FS_v) under monotonic loading show uplifting at their center. However, the footings experience accumulated settlement when it comes to shaking from earthquakes. The settlement values for PGA=0.6g earthquake intensity for both safety factor cases are more than for the PGA = 0.1g case.

REFERENCES

Algie, T. B., Pender, M., Orense, R., & Wotherspoon, L. (2010). *Dynamic field testing of shallow foundations subject to rocking.* Proceedings of 2010 New Zealand Society for Earthquake Engineering Conference, 26-28.

Anastasopoulos, I., Gazetas, G., Loli, M., Apostolou, M., & Gerolymos, N. (2010). *Soil failure can be used for seismic protection of structures.* Bulletin of Earthquake Engineering, 8(2), 309-326.

Anastasopoulos, I., Kourkoulis, R., Gelagoti, F., & Papadopoulos, E. (2012). *Metaplastic Rocking Response of SDOF Systems on Shallow Improved Sand: an Experimental Study.* Soil Dynamics and Earthquake Engineering, 40, 15-33.

Antonellis, G., & Panagiotou, M. (2014). *Seismic Response of Bridges with Rocking Foundations Compared to Fixed-Base Bridges at a Near-Fault Site.* Journal of Bridge Engineering, 19(5), 04014007.

Bowles, J. E. (1977). *Foundation Analysis and Design.* McGraw-Hill.

Chatzigogos, C. T., Figini, R., Pecker, A., & Salençon, J. (2011). *A macroelement formulation for shallow foundations on cohesive and frictional soils.* International Journal for Numerical and Analytical Methods in Geomechanics, 35(8), 902-931.

Deng, L., Kutter Bruce, L., & Kunnath Sashi, K. (2012). *Centrifuge Modeling of Bridge Systems Designed for Rocking Foundations.* Journal of Geotechnical and Geoenvironmental Engineering, 138(3), 335-344.

Gajan, S., & Kutter Bruce, L. (2008). *Capacity, Settlement, and Energy Dissipation of Shallow Footings Subjected to Rocking.* Journal of Geotechnical and Geoenvironmental Engineering, 134(8), 1129-1141.

Gazetas, G. (2015). *4th Ishihara lecture: Soil–foundation–structure systems beyond conventional seismic failure thresholds.* Soil Dynamics and Earthquake Engineering, 68, 23-39.

Gelagoti, F., Kourkoulis, R., Anastasopoulos, I., & Gazetas, G. (2012). *Rocking isolation of low-rise frame structures founded on isolated footings.* Earthquake Engineering & Structural Dynamics, 41(7), 1177-1197.

Housner, G. W. (1963). *The behavior of inverted pendulum structures during earthquakes.* Bulletin of the Seismological Society of America, 53(2), 403-417.

Ko, K.-W., Ha, J.-G., Park, H.-J., & Kim, D.-S. (2018). *Soil-Rounding Effect on Embedded Rocking Foundation via Horizontal Slow Cyclic Tests.* Journal of Geotechnical and Geoenvironmental Engineering, 144(3), 04018004.

Kourkoulis, R., Anastasopoulos, I., Gelagoti, F., & Kokkali, P. (2012). *Dimensional Analysis of SDOF Systems Rocking on Inelastic Soil.* Journal of Earthquake Engineering, 16(7), 995-1022.

Panagiotidou, A. I., Gazetas, G., & Gerolymos, N. (2012). *Pushover and Seismic Response of Foundations on Stiff Clay: Analysis with P-Delta Effects.* Earthquake Spectra, 28(4), 1589-1618.

Sharifzadeh Asli, M., Mir Mohammad Hosseini, S. M., & Jahanirad, A. (2018). *Effect of soil reinforcement on rocking isolation potential of high-rise bridge foundations.* Soil Dynamics and Earthquake Engineering, 115, 142-155.

Sharifzadeh Asli, M. (2018). *Experimental study of effective factors on bed soil improvement in rocking isolation.* PhD. Dissertation. Amirkabir University of Technology, Tehran, Iran.

Torabi, H., & Rayhani, M. (2014). *Three dimensional Finite Element modeling of seismic soil–structure interaction in soft soil.* Computers and Geotechnics, 60, 9–19.

Tsatsis, A., & Anastasopoulos, I. (2015). *Performance of Rocking Systems on Shallow Improved Sand: Shaking Table Testing [Original Research].* Frontiers in Built Environment, 1(9).